Norway grants

Ammonia as carbon free fuel for internal CombusTion engIne driVen AgriculTural vEhicle

ACTIVATE

Work Package 5
Deliverable Report

Topic: D5.6

Report on comparative analysis of the validated environmental impact of ACTIVATEngine and reference CI engine

Programme operated by: NCBR National Centre for Research and Development

Project consortium: Silesian University of Technology, NTNU Norwegian University of Science and Technology, LOGE, University of Agriculture in Krakow

1 Executive summary

This report concludes major findings of the environmental impact of the validated ACTIVATEngine technology obtained by the means of Life Cycle Assessment (LCA) and thermo-ecological analysis (TEC). The assessments compare the ammonia-fueled vehicle versus reference CI diesel tractor considering various ammonia sources in terms of exploitation of the vehicle in the fruit orchard, in line with the previous deliverable reports, conducted within the WP4. The work is based on the experimental data measured in the SUT laboratory. LCA for Experts (GaBi) software was used to perform the LCA with the ReCiPe 2016 v1.1 method used for the Life Cycle Impact Assessment. The assessment indicates that producing ammonia via renewable-powered electrolysis could reduce climate change impact by about 15% compared to diesel. Limited decarbonization effect is due to high volumes of emitted N2O. Concurrently, the results present a heightened environmental risk to human health and ecosystem quality. These findings are primarily due to NOx and ammonia emissions. Optimizing engine performance and exhaust treatment in terms of these emissions could lead to greater benefits. From a thermo-ecological standpoint wind-powered ammonia synthesis is identified as the most favorable option, suggesting a lower long-term depletion of non-renewable resources.

2 Life Cycle Assessment

2.1 Goal and scope

The LCA assessment performed for this project is a cradle-to-grave type of the analysis i.e. it includes all stages from extraction of the materials to the end of life, following the phases presented in the Figure 2.1. The objective was to compare the environmental impacts of diesel- and ammonia-fueled mini tractor during its operation in an orchard. Consequently, the selected functional unit is the hectare-year of the tractor's operation. A case study focusing on a fruit orchard was chosen, primarily due to the small size of the analyzed single-cylinder Lifan C186F engine, which has a displacement of 418 cm^3. This choice allows for a realistic assessment of the tractor's operation

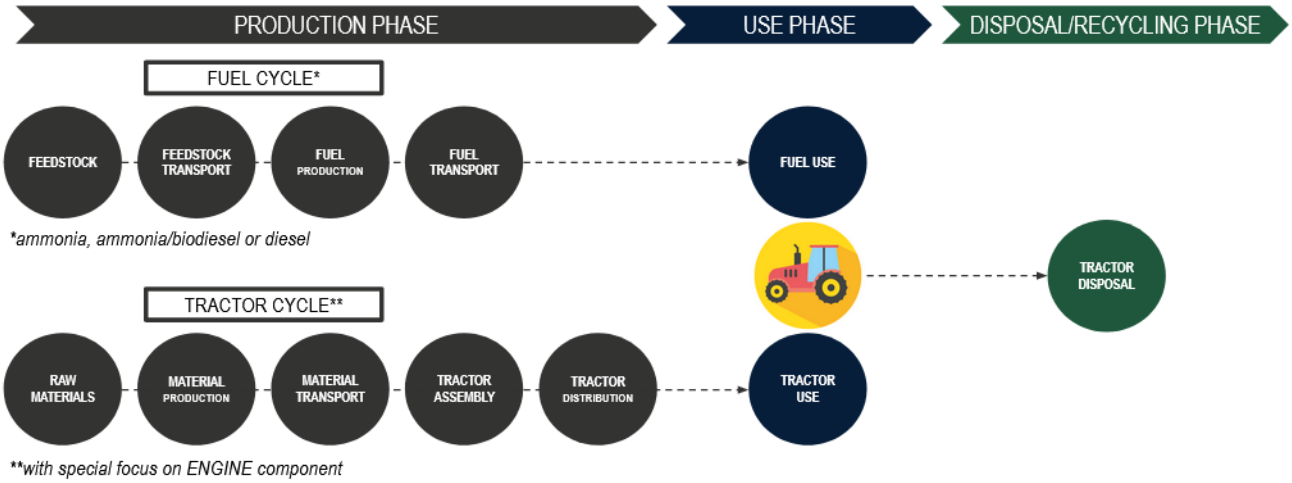

Figure 2.1: LCA scope.

2.2 Life Cycle Inventory

The LCA model consists of a set of processes, built in the LCA for Experts (GaBi) software, with the respective phases modeled using an input-output approach. The details regarding the data and processes, which constitute the Life Cycle Inventory, are elaborated in Table 2.1. This study operates under the assumption that the industry-specific data derived from the LCA for Experts (GaBi) database (Sphera's Managed LCA Content) accurately mirrors real-world scenarios. The descriptions presented in the Table 2.1 for the aggregated processes are sourced directly from the software. The LCA does not focus on a particular case study or country; instead, it aims to represent the current state focusing mostly across the European region.

Table 2.1: Overview of LCA model phases.

Process	Source	Description
Farm tractor production	Software database	An aggregated process provides an estimate of farm tractor production, derived from industry data, based on material composition. Maintenance of the tractor over 5 years period is also included. The dataset is representative for a global region. For ammonia-based vehicle a 10% of mass increase is assumed.
Diesel production	Software database	An aggregated process treats the diesel as one of the co-products from a refinery plant that includes a set of specific processes: distillation, desulfurization, cracking alkylation and others. The contribution of diesel is determined based on the mass allocation and the net calorific value of the products. The dataset is representative for Europe.
Biodiesel production	Literature and software database	The transesterification process was modeled using literature inputs regarding the energy and material requirements [1], complemented by upstream processes assumed from the software database. The study [1] analyzed three transesterification methods: the alkali-catalyzed process, the acid-catalyzed process, and the supercritical methanol process using propane as a co-solvent. This work considers the last method as the most environmentally benign option. Refined rapeseed oil is used as the feedstock, and its production process, including cultivation, harvesting, processing, milling, and refining, was analyzed using an aggregated process from the software database, based on data from the German market. Using Eurostat statistics from 2022, which detail the quantity of total transported goods and their associated travel distances, the transportation distance between the biorefinery and the end user was determined, using a mass allocation for 1 tonne of goods. This yielded a distance of 140.5 km of biofuel transportation. Truck transport was assumed.
Ammonia production	Literature and software database	The following cases are considered: Grey ammonia - utilizing hydrogen from steam methane reforming, with the process sourced from the software database and applicable to Europe. Blue ammonia - utilizing hydrogen from steam methane reforming with carbon capture and storage, also based on the software database and relevant to Europe. Green ammonia - produced using hydrogen from electrolysis, with the electrolysis definition derived from the literature [2] and upstream processes from the software database. PV and wind are considered as sources of electrical energy. Pink ammonia - similar to green ammonia, but with nuclear energy as the source for hydrogen production. For all cases, the sources of electrical energy generation and the nitrogen production via air separation unit are based on the European industry.

Tractor operation	Experiments	The dataset is derived from experimental measurements of the engine conducted in the SUT laboratory and is considered to have global validity due standardized nature of the testing procedures. A thorough discussion regarding this phase is presented in the subsequent sub-chapter 2.2.1.
Tractor utilization	Software database	The end-of-life phase, included in tractor utilization, is represented by an aggregated process. This process involves shredding the vehicle body, which includes partial disassembly of used parts prior to shredding. The dataset for this phase is based on the German market

2.2.1 Tractor operation phase

The operational phase of the tractor aimed at determining the emissions occurring due to the utilization of the tractor, working on the one hectare of orchard over one year period. The emissions from a detailed working cycle has been determined using the following method.

First, a set of activities performed on the orchard over one year were determined. These are summarized in Table 2.2. A case study of apple orchard was assumed, a set of activities was based primarily on the [3].

Table 2.2: Orchard management activities and their frequency.

Activity	Frequency during a year
Branch and leaves sweeping and raking	2
Mechanical weed removal	1
Grass mowing	8
Pruning	2
Fruit harvest	1
Tree fertilizing	4
Insecticide and fungicide application	20

In the second step, an orchard CAD model, in scale, was developed to determine how each activity would be executed within the orchard. To illustrate it, the scheme of spraying can be seen in Figure 2.2. In an analogous way, schemes for all activities were drawn. Concurrently, a theoretical gearbox operation model was determined. The idea was to establish the engine's condition i.e. shaft's torque and rpm, while moving along the orchard. Having determined these two parameters, these conditions could be reflected on the test rig. Figure 2.3 depicts the gearbox operation, factoring in the tractor's movement from the storage unit to the orchard over an intervening dirt road. The names used in the legend regard the gear and speed, e.g. G1/S2 stands for gear 1, speed 2 km/h.

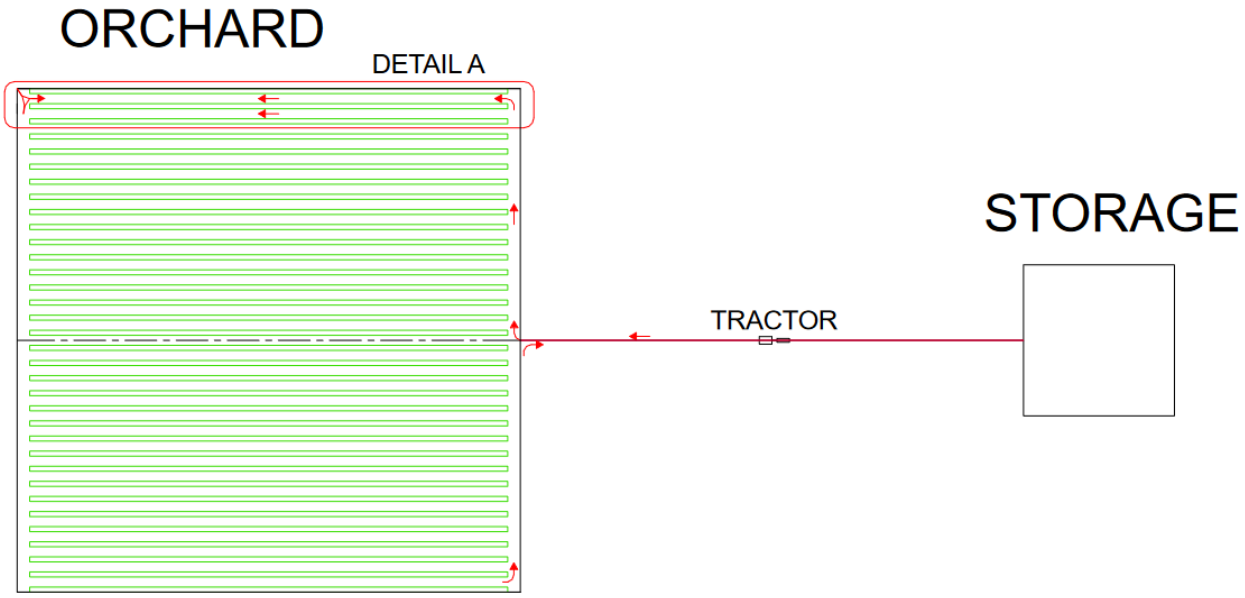

Figure 2.2: Sweeping scheme – movement of the tractor along the orchard.

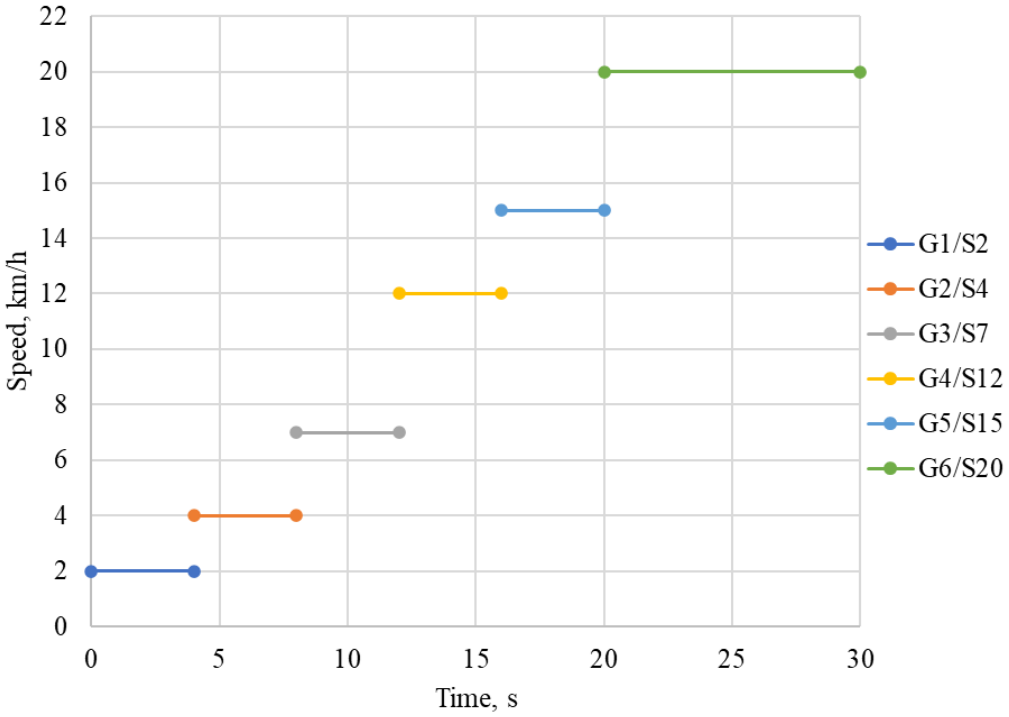

Figure 2.3: Steady point approximation of storage – orchard distance in terms of driving cycle.

Having established the working point which constitutes to the road movement (e.g. gear 1, average speed 2 km/h, at the beginning), the engine's power was calculated based on the tractor's characteristics (transmission losses depending on the gear), rolling resistance, and a type of operation. For instance, during grass mowing, a mower is attached to the tractor, whereas for sweeping, a sweeper is affixed. Since the two devices have different weights, they cause different rolling resistance. Additionally, the engine's condition differ depending on the mode, i.e. switched on sweeper causes higher torque of the shaft than in case of switched off mode. For a diesel reference case, it was determined that at all shaft's speeds, the maximum applied torque (on the electrical machine) was equal to 17 Nm. Therefore, it was possible to determine the maximum load of the shaft at all speeds. For example, for switched on sweeper mode the shaft's speed was calculated based on the typical operating speed of the device with a mini tractor whereas the power was assumed to be the maximum possible value (corresponding to the mentioned 17 Nm torque). Such approach is a conservative perspective i.e. turning the device assumes that turning the closes the energy balance of the engine.

To illustrate this approach, Figure 2.7 aggregates the power of the shaft (Ne, kW) plotted versus cumulative value of time for a sweeping activity. It considers moving of the vehicle of storage and moving on the road, making the turn, traveling through the vertical alley, making a turn to the horizontal alley, moving through the horizontal alley (with switched on sweeper, two times), and then going back to the storage unit. For a simplification, in the figure going through the horizontal alley is shown once (two times per alley i.e. both sides), however in the considered analysis this is repeated for the number of the horizontal alleys considered (and then there is moving back to the storage unit).

Finally, all orchard activities were broken-down into sub-activities such as moving along the road, making a turn, moving along the alley etc., and analyzed from the perspective of engine's conditions. The goal was to define all working points in respect to all activities. The characteristics of the devices were based on the technical card of the equipment suited to work with the considered mini tractor. Set of agricultural devices with their weights and the speeds assumed while performing the activity are shown in the Table 2.3. Ultimately, the emissions and fuel consumption at respective working points have been integrated over distances known from the CAD model of the orchard, in respect to all activities elaborated in 2.2. The measured values were interpolated to match the points calculated from this definition of the working cycle.

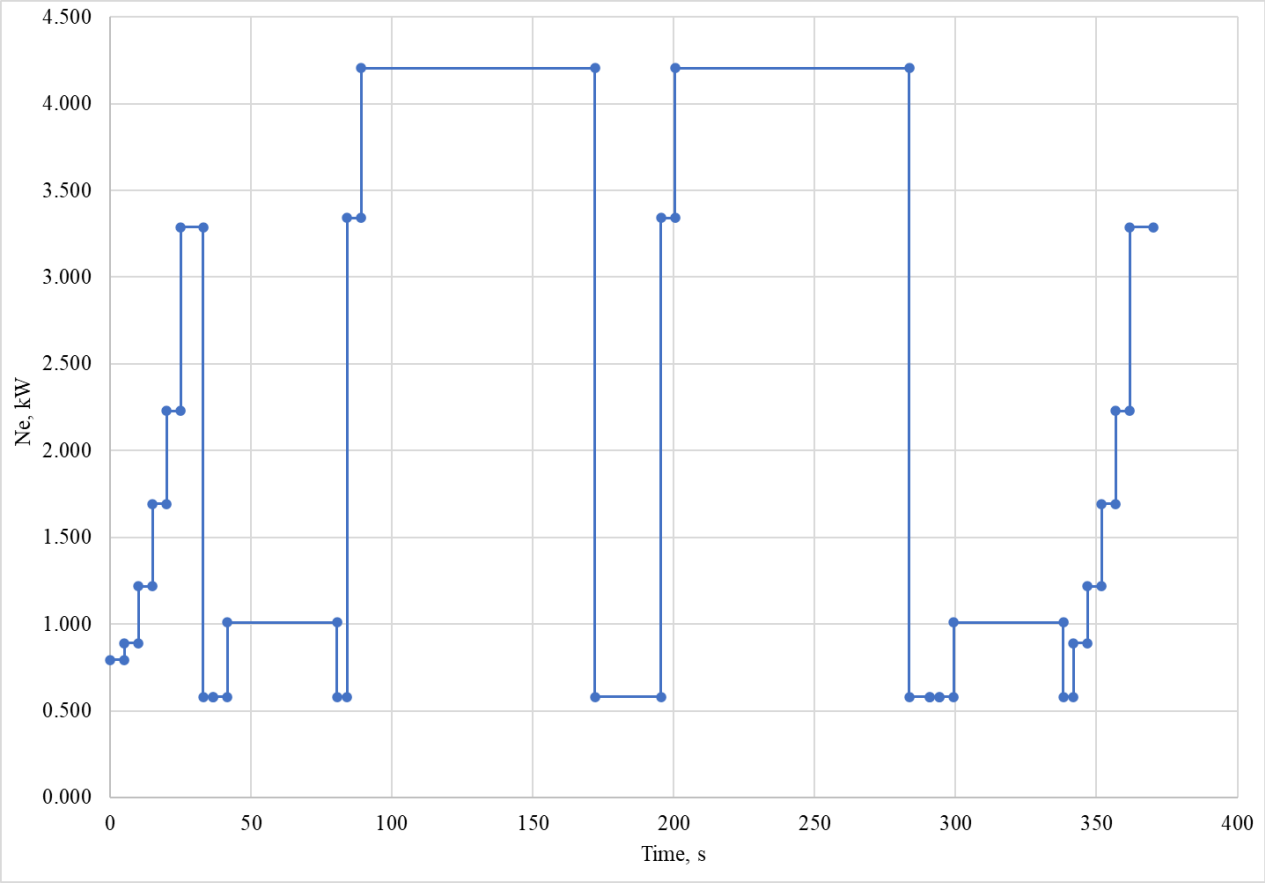

Figure 2.4: Power of the engine versus cumulative time for the sweeping activity (simplified).

Table 2.3: List of agricultural devices working with the tractor with their weights and operating speeds.

Equipment	Mass	Speed of tractor while operating the equipment
Hooked sweeper	80 kg	4 km/h
Side hoe	100 kg	4 km/h
Rotary mower	50 kg	6 km/h
Sprayer	180 kg (+ mass of the full tank 400 kg that decreases throughout spraying activity)	4 km/h
Trailer	80 kg (+mass of the full trailer 500 kg)	1 km/h (going through the alley)

The measured values during the tests included fuel consumption, CO2, CO, CH4, C2H6, C2H4, C6H14, H2O, N2O, NO, NO2, SO2, NH3, HCL, HF, PM10. The tests performed in the WP5 regarded the ammonia introduced to the cylinder through direct injection, using biodiesel as a pilot fuel. It has been mentioned that for a diesel reference case, it was determined that at all shaft's speeds, the maximum applied torque (on the electrical machine) was equal to 17 Nm. This was not possible to achieve with ammonia fuel during the direct injection test, however it was accomplished for port injection, performed previously in the WP2, and analyzed in the WP4 (shown in D 4.2). The engine's map, understood as a set of measured points, for the two cases, in the form of energy balance is presented in the Figure 2.11. The BP stands for the brake power on the shaft, Q_{exh} indicates the energy of exhaust (physical enthalpy), and the Q_{lost} is the energy lost to the environment. It is seen that direct injection test allowed for maximum 12 Nm torque at 2000 rpm, and only a low torque above this rpm. Direct injection, while offering superior control, struggles with efficient fuel-air mixing at higher RPMs, leading to potential combustion issues. In contrast, port injection achieves a more uniform mixture, beneficial for efficient combustion. This can lead to issues with incomplete combustion or uneven fuel distribution. Port injection is characterized by a more homogeneous air-fuel mixture. Notably, at similar operating points, direct injection exhibits higher exhaust energy than port injection, indicating less efficient combustion. For instance, at 8 Nm torque and 2100 rpm for port injection, the exhaust energy is equal to 2645 W. For direct injection, at 8 Nm and 2000 rpm, this exhaust energy is equal to 3825 W. Although the RPMs aren't identical, the substantial difference in exhaust energy underscores this inefficiency in direct injection. This is further seen when plotting the comparison of efficiency between the port and direct injection test, as seen in the Figure 2.12. For instance, at 2100 rpm and 12 Nm torque for port injection, the thermal efficiency is equal to ca. 29%, whereas at 2000 rpm and 12 Nm torque for direct injection test, it is equal to 26%. On average, thermal efficiency of direct injection engine is lower by ca. 2-3 percentage points compared to the port injection. Apart from the specific differences between the port and direct injection fueling strategies, this result should be considered from the perspective of design of the test. The port injection test took place in March, at much lower air temperature, compared to the direct test which was performed during summer period. Both tests took place in Gliwice, Poland at SUT laboratory. Warm air is associated with lower air density which results in lower volume of air entering the cylinder. This means less oxygen is available for combustion per unit volume of air intake, and the optimization of direct injection strategy might require additional calibration. Additionally, the port injection was performed in such a way that the 4 Nm torque was derived on a basis of pure biodiesel, and the increase in torque was achieved by addition of the ammonia into the intake manifold. At low load of the engine this means that pure biodiesel is compared to modified biodiesel with ammonia engine which could favor the pure biodiesel scenario as the engine was originally designed for combustion of pure diesel fuel. To incorporate the direct injection test into the Life Cycle Impact Assessment (LCIA), the following assumption is used: if the value obtained from the definition of the working cycle is higher than the one measured for the direct injection, a port injection data are used. As such, the considered ammonia-fueled vehicle should be treated as a hybrid of direct and port injection model. This issue arises from the fact that the working cycle has been determined to reflect the real operation of the vehicle; adjusting the working cycle to match the direct injection test would allow to avoid combining to different sets of data, however this approach was determined to lower the quality of the analysis since it would not reflect the typical operations performed with the vehicle.

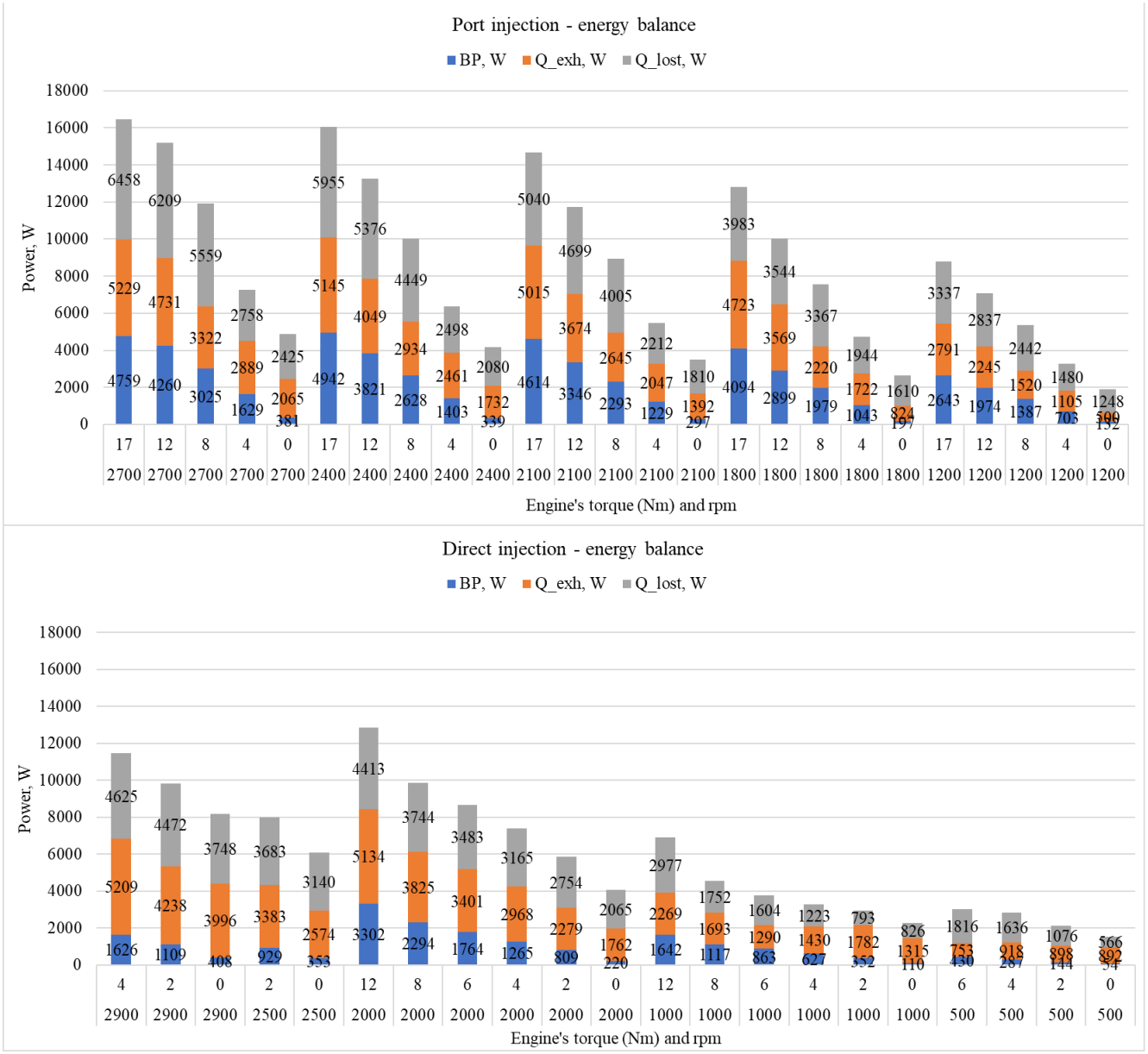

Figure 2.5: Energy balance comparison for port and direct injection test.

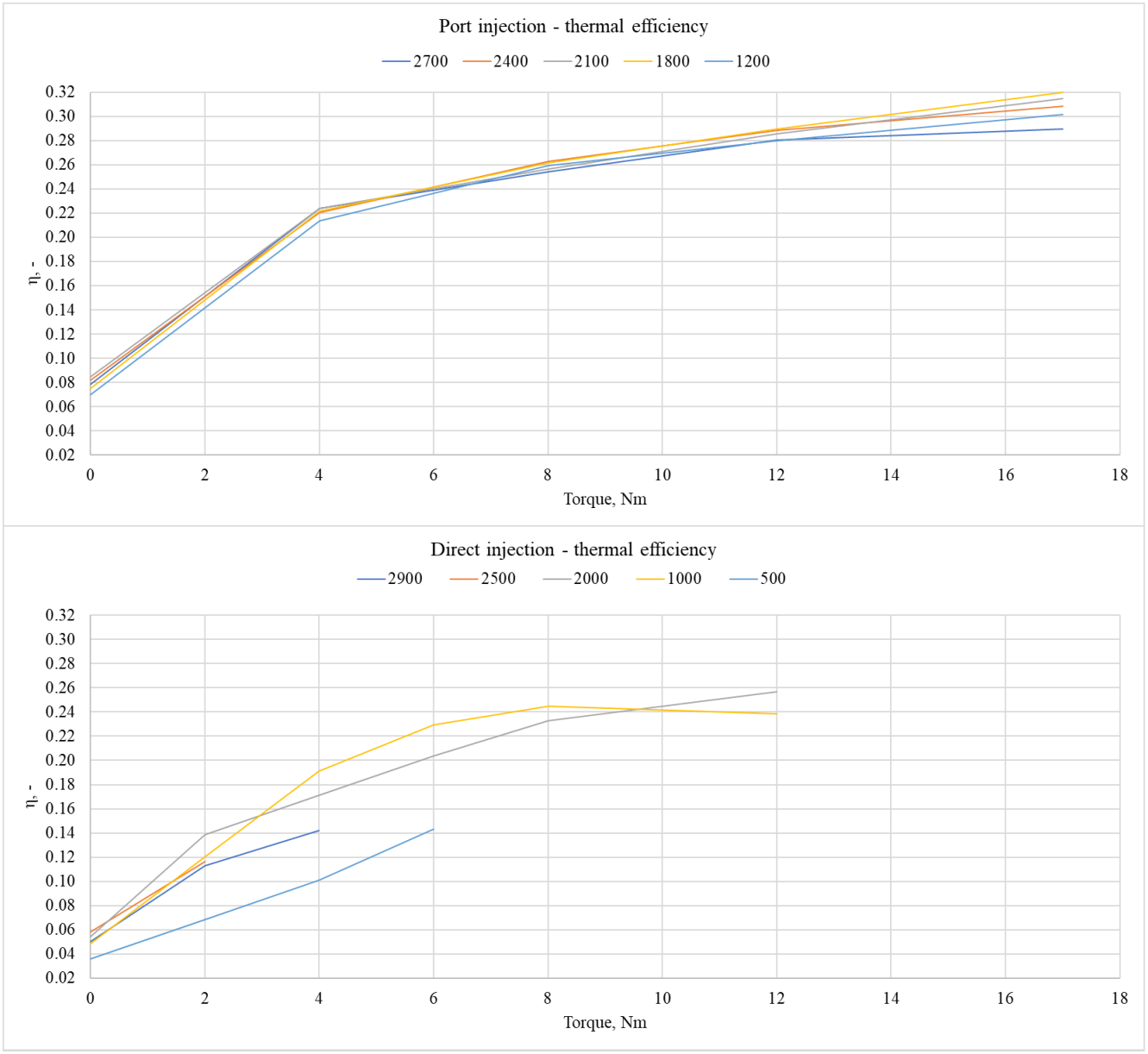

Figure 2.6: Thermal efficiency comparison for port and direct injection test.

2.3 Life Cycle Impact Assessment and Interpretation

2.3.1 Impact Categories

ReCiPe 2016 v1.1 method has been used to LCIA which includes 18 midpoint indicators and 3 endpoint indicators. Referring to the D 4.2, a short description of respective categories can be repeated [4]:

1. Midpoint climate change – measured in kg CO2 eq., this category quantifies climate change impact due to greenhouse gas emissions, which affect the Earth's radiative forcing capacity, leading to an increase in global mean temperature.

2. Midpoint fossil depletion – referred to as kg oil eq., measure of the reduction in future availability of fossil fuels caused by exploitation of these fuels in regard to the unit of product (production of 1 MJ of ammonia in this case).

3. Midpoint freshwater consumption – referred to as m^3, defining the measure of water exploitation referred to evaporation, incorporation into products and by-products or disposed to sea causing the loss in availability of freshwater for ecosystems.

4. Midpoint stratospheric ozone depletion – referred to as kg CFC-11 eq., it regards the Ozone Depletion Potential (ODP) quantifying the amount of ozone depleting by the substance.

5. Midpoint ionizing radiation – measure of collective exposure dose caused by the emission of radionuclide, referred in the kBq Co-60 eq. to air.

6. Midpoint fine particulate matter formation – referred to as PM2.5 eq., defining the health damage due to the exposure to fine dust.

7. Midpoint photochemical ozone formation – measure of intake of ozone by humans for human health category and by plants for ecosystem category, expressed in kg NOx eq.

8. Midpoint terrestrial acidification – measure of change in acidity in soil due to emission of inorganic substances (sulphates, nitrates and others), referred to as kg SO2 eq.

9. Midpoint freshwater eutrophication – measure of eutrophication caused by the discharge of nutrients into soil and freshwater, referred to as kg P-eq. (phosphorus eq.) to fresh water.

10. Midpoint marine eutrophication – measure of runoff and leach of plant nutrients from soil and discharge into rivermarine and marine systems, referred to as kg N eq. (nitrogen eq.).

11. Midpoint toxicity – this term regards the four midpoint categories: human toxicity cancer, human toxicity non-caner, marine ecotoxicity and terrestrial ecotoxicity. Human toxicity accounts for the measure of human intake of a chemical and accumulation in a human food chain in regard to carcinogenic and non-carcinogenic substances. Marine and terrestrial ecotoxicity consider the increase in concentration of the chemicals leading to disappeared fraction of species. They are expressed in kg 1.4-dichlorobenzene-equivalents (1.4 DB eq.).

12. Midpoint land use – measure of land transformation, occupation and relaxation referred to as annual crop eq.

13. Midpoint mineral resource scarcity – measure of resource extraction leading to ore grade decrease referred to as kg Cu eq.

14. Endpoint human health – referred to as DALYs (disability adjusted life years) representing the years that are lost by a person due to the disease or accident.

15. Endpoint ecosystem quality – referred to as species year as time-integrated species loss representing such loss at local scale.

ReCiPe 2016v1.1 method recognizes also the third endpoint category i.e. resource scarcity which represents the extra costs involved in future mineral and fossil resource extraction. It is calculated based on the average annual costs for cooper, crude oil, hard coal and natural gas. Since the primary aim of this LCA was to assess the environmental impacts, it has been omitted due to its economic-based nature.

2.3.2 Validated LCA results

The results for climate change (midpoint category), human health and ecosystem quality (endpoint categories) for validated LCA result are presented respectively in Figures 2.7, 2.9 and 2.10. Reference diesel engine is compared to ammonia variants. The experimental data for the operation phase regard the direct injection test performed on the engine installed on the test rig. The biogenic carbon is considered in the analysis since the biodiesel production is characterized by negative carbon emissions (rapeseed cultivation included as explained in the 2.1). To visualize the results from Figure 2.7 in a single score, a Figure 2.8 has been plotted. 'Fuel production' term in the figures regard the production of a pilot fuel, biodiesel.

The results on the climate change category do not indicate a strong decarbonization effect of the ammonia-fueled tractor. This is due to two primary reasons: the conventional pathway of ammonia production, which is responsible for high GHG emissions, and the fact that the operation phase of the ammonia-fueled vehicle emits 25% more GHG compared to the diesel case. This outcome is attributed to the fact that the measurements for a whole engine map (i.e. different shaft's speeds and torque) were performed without the exhaust treatment SCR unit. As a consequence, large quantities of NOx as well as the nitrous oxide, N2O, which is characterized by the 100-year global warming potential equal to 298, were measured. Considering the negative carbon emissions of biodiesel production and electrical energy source with the low GHG emissions, green and pink scenarios allow for achieving ca. 15% reduction on climate change compared to the diesel reference case. High emissions of NOx are apparent in the results on human health where the operation phase has the dominant contribution for ammonia-fueled variants and causes considerably higher impact compared to the diesel case. Effect of high NOx is further visible in the results on ecosystem quality where the operation phase for ammonia-based cases is high compared to diesel. Additionally, both biodiesel and ammonia production pathways considerably impact the result on the ecosystem quality, with the highest value obtained by the PV based ammonia scenario.

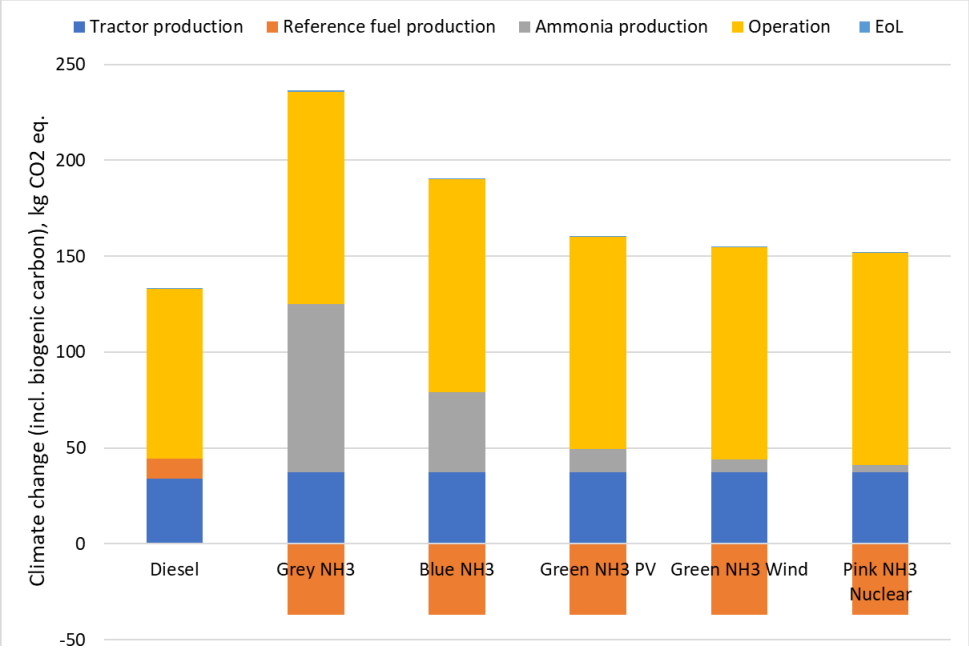

Figure 2.7: Climate change results in regard to life cycle phases.

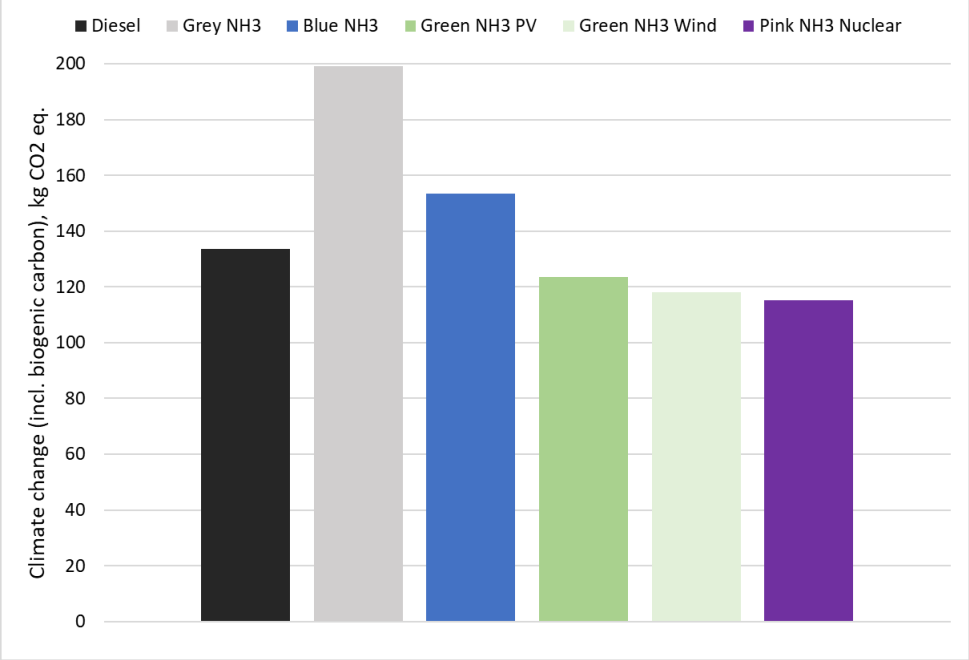

Figure 2.8: Climate change results in a single score.

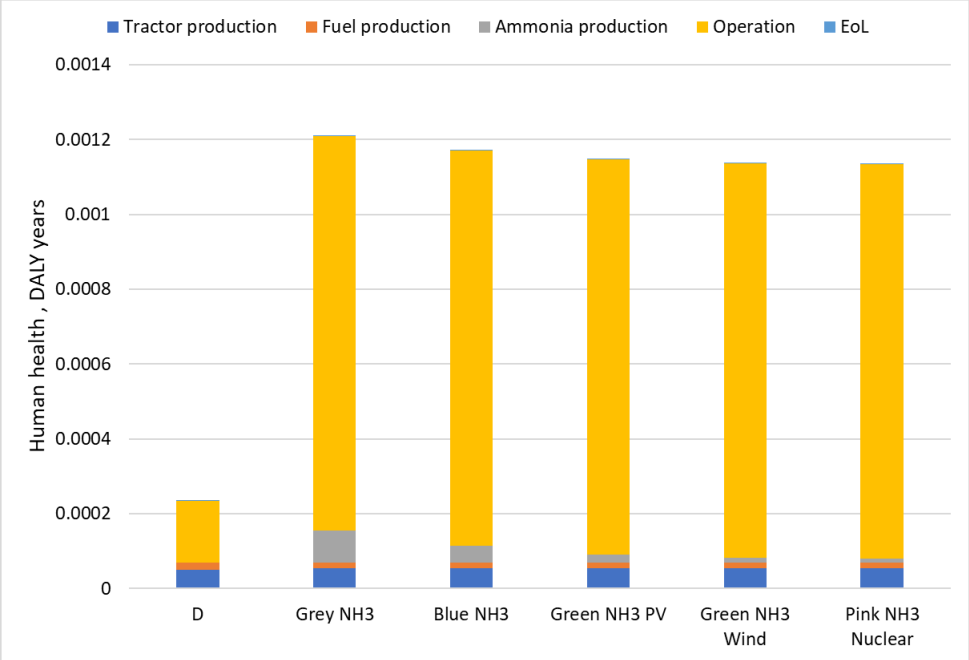

Figure 2.9: Human health results in regard to life cycle phases.

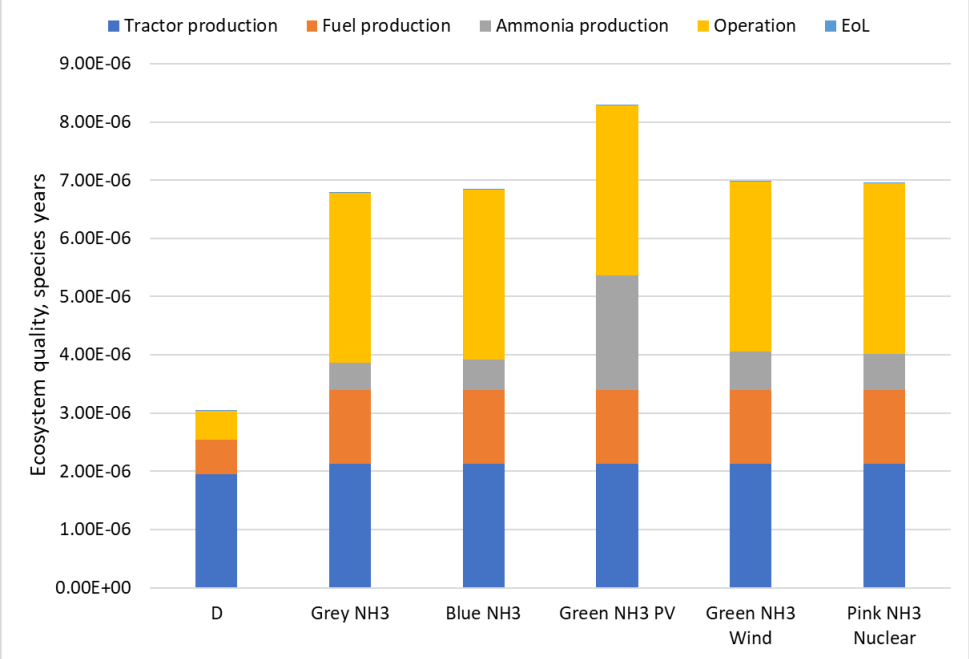

Figure 2.10: Ecosystem quality results in regard to life cycle phases.

The results on other midpoint categories are presented respectively in Figures 2.11, 2.12, 2.13, 2.14, 2.15. The major trends could be summarized in the following way:

1. The highest impact on fossil depletion is achieved by the pink NH3 scenario with the ammonia production phase as the strongest contributor.
2. The highest impact on freshwater consumption is achieved by the pink NH3 scenario with pilot fuel and ammonia production phases as the strongest contributors.
3. The impact on fine particulate matter formation is similar for all ammonia scenarios and it is considerably bigger compared to diesel due to larger NH3 and NO2 presence in the exhaust.
4. The highest impact on freshwater ecotoxicity is achieved by the pink NH3 scenario with biodiesel production phase as the strongest contributor.
5. The impact on freshwater eutrophication is similar for all ammonia scenarios and it is considerably bigger compared to diesel with the biodiesel production phase as the strongest contributor.
6. The highest impact on human toxicity, cancer is achieved by the green NH3 wind scenario with ammonia production as the strongest contributor.
7. The impact on human toxicity, non-cancer is similar for all ammonia scenarios and it is considerably bigger compared to diesel with the biodiesel production phase as the strongest contributor.
8. The highest impact on ionizing radiation is achieved by the pink NH3 scenario with ammonia production as the strongest contributor.
9. The impact on land use is similar for all ammonia scenarios and it is considerably bigger compared to diesel with the biodiesel production phase as the strongest contributor.
10. The impact on marine ecotoxicity is rather similar for all ammonia scenarios with peak values obtained by green NH3 PV and pink NH3. It is bigger compared to diesel with the biodiesel and ammonia production phases as the strongest contributors.
11. The impact on marine eutrophication is rather similar for all ammonia scenarios with peak value obtained by grey NH3. It is considerably bigger compared to diesel with the biodiesel production phase as the strongest contributor.
12. The impact on metal depletion is rather similar for all ammonia scenarios with peak value obtained by green NH3 wind. It is considerably bigger compared to diesel with the biodiesel production phase as the strongest contributor.
13. The impact on photochemical ozone formation, ecosystems is similar for all ammonia scenarios and it is bigger compared to diesel with the operation phase as the strongest contributor.
14. The impact on photochemical ozone formation, human health is similar for all ammonia scenarios and it is bigger compared to diesel with the operation phase as the strongest contributor.
15. The impact on stratospheric ozone depletion is similar for all ammonia scenarios and it is considerably bigger compared to diesel with the operation phase as the strongest contributor.

16. The impact on terrestrial acidifcation is similar for all ammonia scenarios and it is considerably bigger compared to diesel with the operation phase as the strongest contributor.

17. The impact on terrestrial ecotoxicity is rather similar for all scenarios apart from green NH3 PV where the ammonia production contributes stronger compared to other ammonia production pathways.

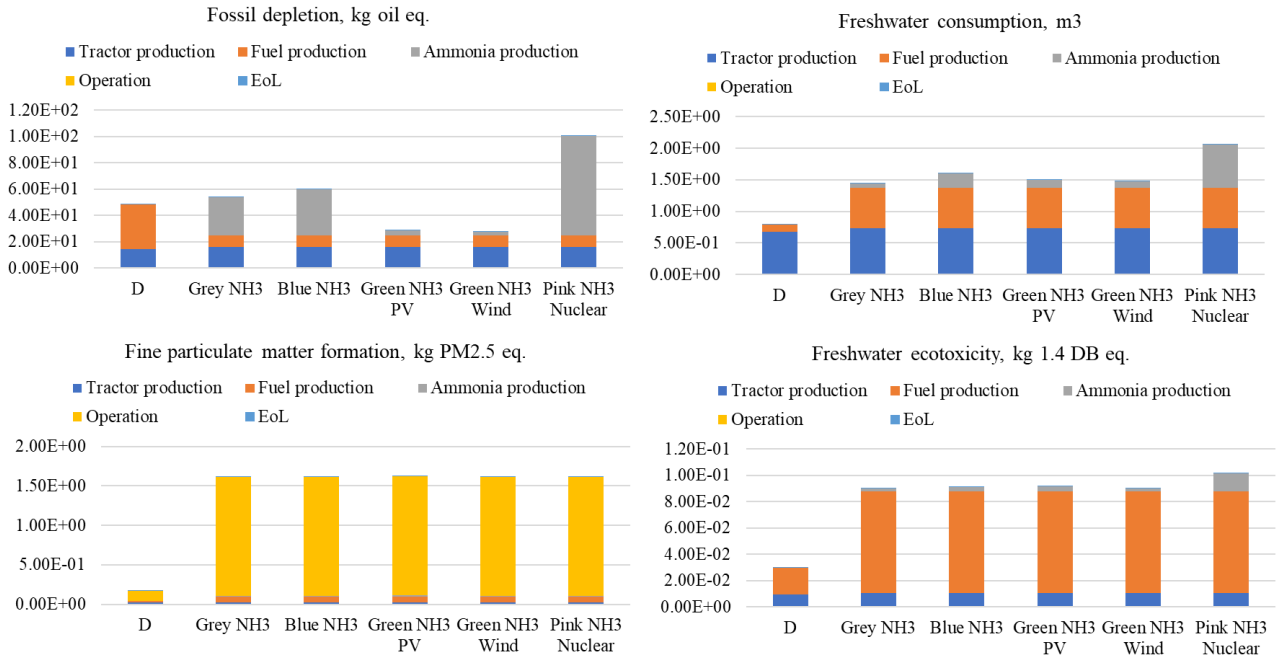

Figure 2.11: ReCiPe midpoint categories results in regard to life cycle phases (1).

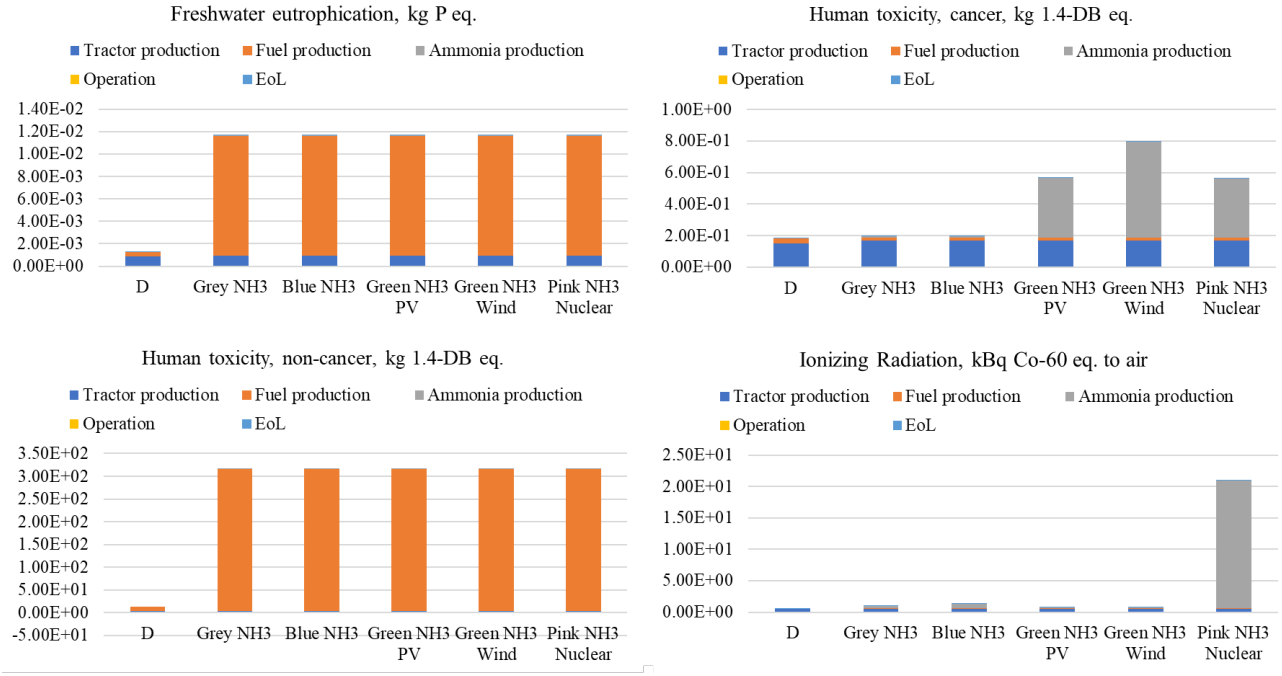

Figure 2.12: ReCiPe midpoint categories results in regard to life cycle phases (2).

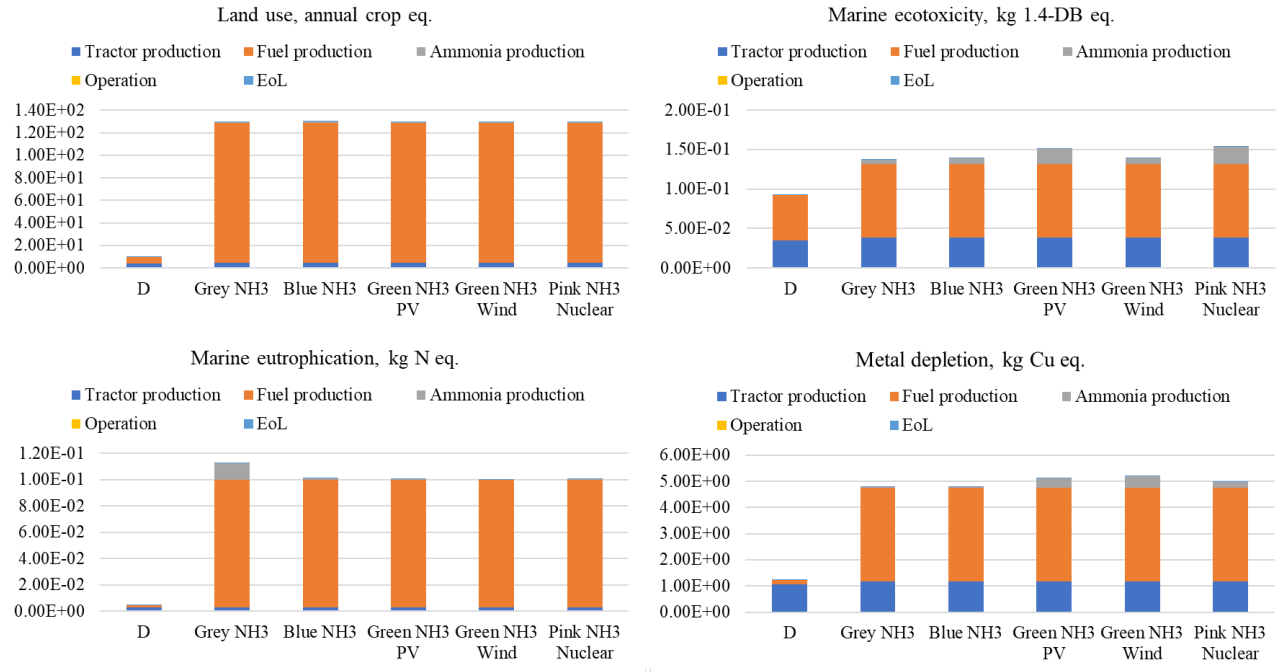

Figure 2.13: ReCiPe midpoint categories results in regard to life cycle phases (3).

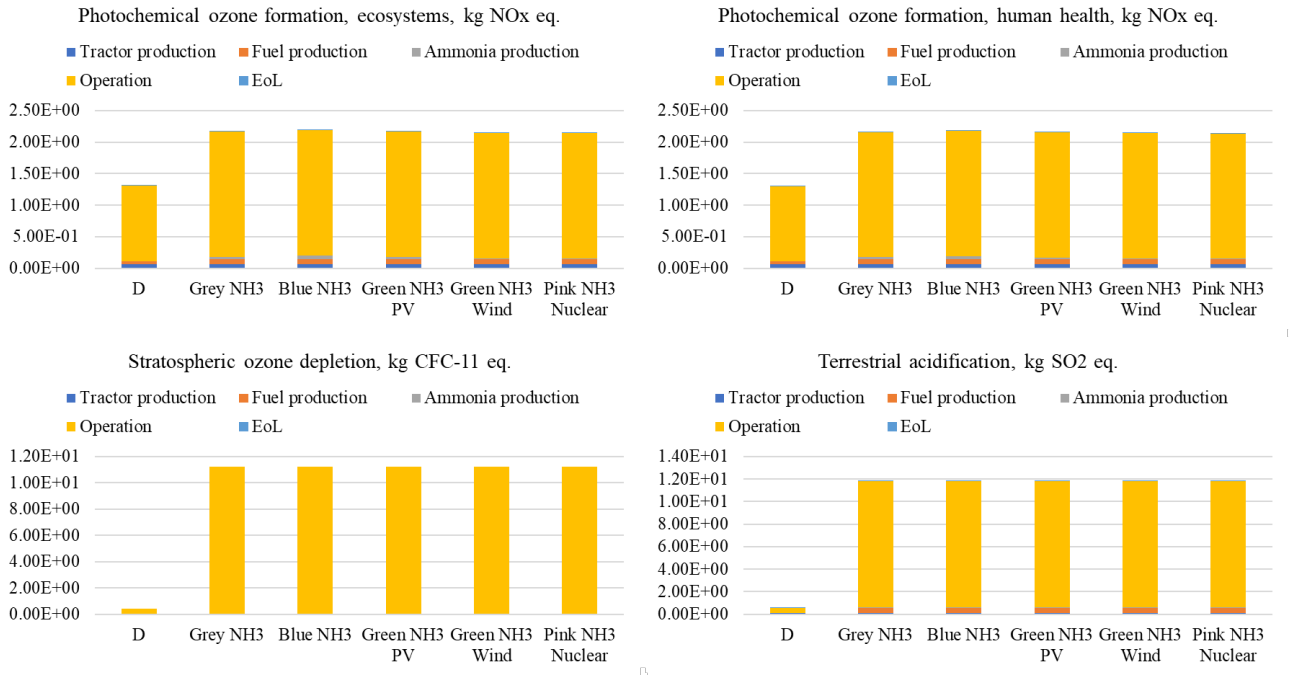

Figure 2.14: ReCiPe midpoint categories results in regard to life cycle phases (4).

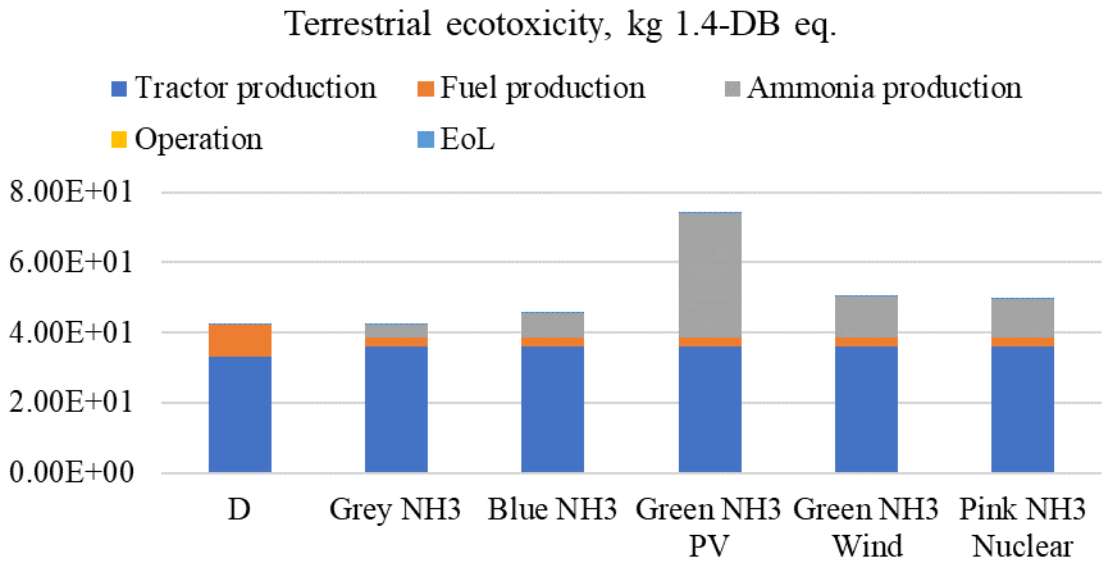

Figure 2.15: ReCiPe midpoint categories results in regard to life cycle phases (5).

High emissions of NOx due to the combustion of ammonia is not unforeseen, therefore several tests with V2O5/SiO2–TiO2 SCR unit were performed and presented in the paper [5]. However, since they have not been conducted for the engine map due to the technical challenges, the precise results for the validated LCA cannot be shown. Still, utilizing the results from the [5] which presented the SCR performance at 1500 rpm between 10 Nm and 17 Nm torque, could be incorporated into the analysis under a simplified assumption that the efficiency of the SCR is a function of the exhaust temperature only. Reduced emissions of NO, NO2 and NH3 were calculated assuming that the SCR works within the measured range of temperature provided in the [5]. The revised results on human health and ecosystem quality are presented in the Figures respectively 2.16, 2.17. The impact of operation phase on both categories was reduced by ca. 20% for both cases which still results in considerably higher impact of ammonia-fueled scenarios compared to diesel. The primary reason for small reduction effect was low decrease in NH3 emissions.

The results are presented for the most environmentally benign ammonia-fueled scenarios; wind and nuclear based ammonia production pathways. The results on climate change including the SCR are not presented since the reduction of N2O by the SCR unit has not been observed [5], and therefore the results on climate change remain the same. This is a common trend, e.g. [6], and therefore a method for reduction of N2O formation should be considered in the future research. SCR construction is not included into the analysis since its mass is small compared to the total size of the engine, and therefore such approach was assessed to be sufficient.

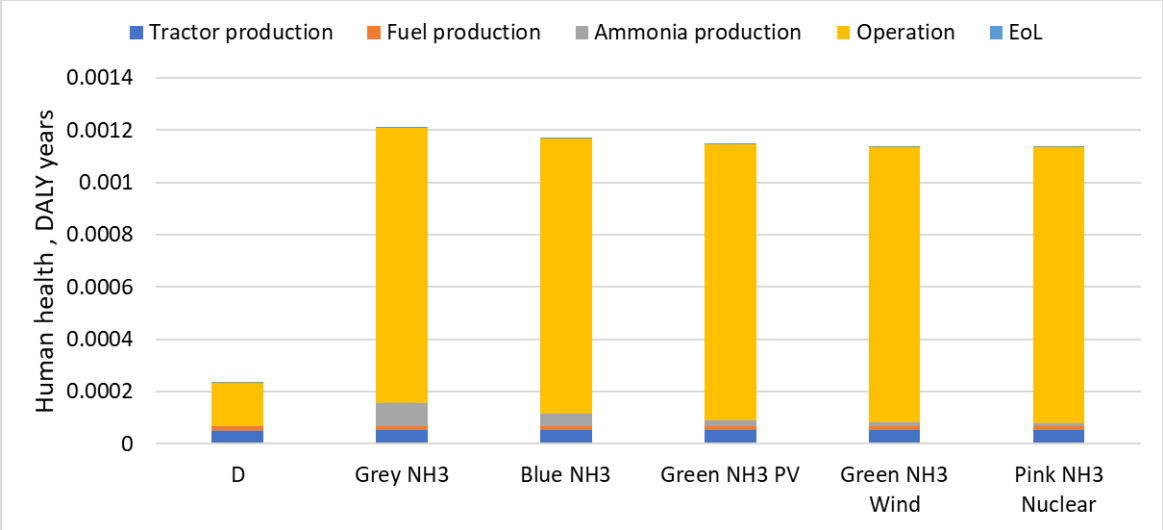

Figure 2.16: Human health results in regard to life cycle phases including SCR.

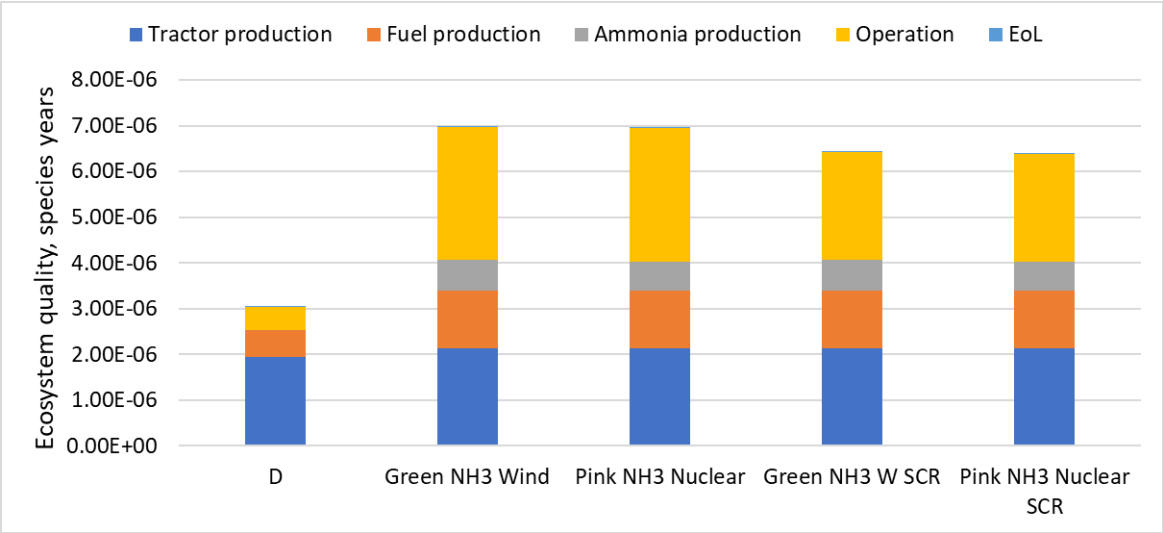

Figure 2.17: Ecosystem quality results in regard to life cycle phases including SCR.

The ACTIVATEngine developed within the project includes a system that was not originally planned; the pneumatic system for ammonia injection into the cylinder. It is not included into the main system boundary presented in the Figure 2.1 since initially the ACTIVATEngine was tested using a pump. Expanding the LCA system by nitrogen production and pressurizing does not impact the overall results considerably; assuming the ratio of nitrogen to ammonia consumption to be 1:2, the increase in impacts for ammonia vehicle scenario follows: 1.26 kg CO2 eq. for climate change, 1.54E-06 daly years for human health, 1.79E-08 species years for ecosystem quality.

Comparing the results presented in this report with those in D 4.2, it is evident that the validated results exclude scenarios involving pure biodiesel or solely port injection fueling options. This exclusion is primarily due to the tested biodiesel being derived from rapeseed oil, a first-generation biofuel. Given the broader environmental and socio-economic concerns, such as indirect land use change and competition with food crops, this type of biofuel is less favored for promotion. While the rapeseed-based biodiesel might demonstrate the lowest climate change impact according to the ReCiPe method, relying solely on these findings could lead to misleading conclusions. The narrow environmental benefit depicted fails to account for the broader negative implications associated with first-generation biofuels. In the D 4.2 report, the biodiesel option was included, as it assumed no oil production impact; the waste vegetable oil was considered an output from an external process, with no environmental impact allocated to it. Data from the port injection was partially used, as explained in the section 2.2.1, sole port injection was not analyzed since the primary goal of this report is to show the ACTIVATEngine performance which is based on the direct injection system.

The measurements performed in the WP5 included also the test of the vehicle on a chassis dynamometer: different speed of the vehicle was investigated while operating the tractor at 6th gear at no additional brake power. Since no load was applied, the amount of power measured on a chassis (power on the wheels) is a measure of a transmission system for the engine to run the mini tractor. This relationship could be used to determine the relationship between the power on the wheels and the indicated power (measured separately), and thus provide an estimation of the transmission losses. Since the calculations for the operation phase of the LCA are based on the set of previously determined relationships between the electrical machine, brake power, and the vehicle's

wheels, these transmission losses were not required to be considered. Given that the tests on the chassis did not include the conditions of the tractor under varying load (and type of operation i.e. gear), they have not been incorporated into the LCA analysis.

The uncertainty of the LCA assessment stems from the quality of the processes included in the software database, as all phases of the LCA, apart from the operation phase, are modeled either directly from the software database or by using literature data, with upstream processes modeled from the database. The quality of the database is ensured through technical and methodological verification, in accordance with the processes' descriptions, and thus they are considered precise. The operation phase is based on measurements that depend on specific equipment. While each device is associated with its own uncertainty, these uncertainties are small, since the devices are designed for such operations. The paper [7] provides comprehensive information regarding the uncertainty of the measured values based on the experimental procedure; however, the calculated values are small as well, and therefore the results are considered reliable.

However, the emissions accounted for in the operation phase may differ from the actual emissions. This discrepancy arises because the emissions, expressed in grams per second (g/s), were calculated based on a carbon balance. This calculation assumes that the exhaust gas behaves as an ideal gas, and that the carbon present in the fuel is fully represented by the carbon components in the exhaust. Treating the exhaust as an ideal gas at high temperature and moderate pressure is a common practice, and hence, the difference arising from treating the exhaust as an ideal gas, rather than a real one, is considered acceptable. Also, there is a possibility of unmeasured carbon components in the exhaust, but their share is likely to be very small thus not affecting the results. Using carbon balance to assess emissions is a standard and accepted approach, which lends credibility to the operation phase's reliability.

Apart from the considered ammonia production pathways, there is also the possibility to produce hydrogen via biomass gasification. However, gasifying biomass is not typically employed to produce hydrogen specifically for ammonia production; rather, the hydrogen obtained from this pathway is more often a co-product of the given biomass processing pathway, primarily targeting biofuel production. Consequently, it is challenging to assess whether this method could facilitate large-scale ammonia production, which is of interest considering the potential use of ACTIVATEngine in the transportation, construction, and agriculture sectors. Nevertheless, assuming the literature's energy requirement [8] for the gasification process alone and utilizing this as an input for ammonia production in terms of ammonia-fueled vehicles, the following results for the environmental categories are obtained: 113.2 kg CO2 eq. for climate change, 0.001126 DALY years for human health, and 6.34E-06 species years for ecosystem quality (with no SCR in the operation phase). Given that these values are close to those associated with green NH3 from wind and pink NH3 from nuclear options, it can be concluded that biomass gasification demonstrates potential environmental benefits. Future research should delve into the cultivation phase impacts, taking into account the variety of biomass types and their availability along with the sustainability.

3 Thermo-ecological cost

Thermo-ecological cost (TEC) serves as a means to compare technologies in terms of their sustainability by measuring exergy. The approach to TEC presented in this report follows the literature [9], [10]. The overall equation can be expressed as follows [9]:

$$TEC = \sum b_s + \sum p_k \zeta_k \tag{1}$$

Here, TEC refers to the value of thermo-ecological cost. The term b_s represents the direct exergy consumption of the s-th non-renewable natural resource, p_k denotes the quantity of k-th waste product, and ζ_k stands for the TEC of the k-th waste product.

The TEC of a k-th waste product is calculated using the following equation [9]:

$$\zeta_k = \frac{Bw_k}{GDP - \sum p_k w_k} \tag{2}$$

where B is the annual domestic consumption of non-renewable resources, GDP is the gross domestic product, p_k is the annual generation of the k-th waste product, and w_k is the monetary harmfulness index of the k-th harmful substance. The variables must be selected for a particular region. In this work, they refer to the Polish market (data for 2021) as an example of an EU country.

Each analyzed technology is considered from a black-box perspective as a whole; that is, the system boundary for calculating the TEC is consistent with that presented in Figure 2.1, which is used for the Life Cycle Assessment analysis. Accordingly, the list of inputs entering the system includes non-renewable energy resources, non-renewable material resources, and uranium resources. The outputs regard the emissions to the air. The first part of the TEC equation presented in Eq. 1 for the s-th resource can be split as shown in Eq. 3:

$$\sum b = \sum b_{fuel} + \sum b_{resource} + \sum b_{nuclear} \tag{3}$$

Here, b_{fuel} represents the chemical exergy of non-renewable fuel resources, $b_{resource}$ is the chemical exergy of exploited non-renewable material resources, and $b_{nuclear}$ denotes the nuclear exergy of exploited uranium resources. From an integrated perspective of the technology, no mechanical or physical exergies are considered; although they appear in each of the processes within the technological chain, they are essentially derived from utilizing the chemical exergy in the previous phase. For instance, the increase in temperature in a stream results from combusting the fuel in a conventional, non-renewable pathway.

The chemical exergy of non-renewable fuel resources is calculated based on the lower heating value (LHV) of the fuel and its empirical coefficient for chemical exergy, as taken from [9]. The chemical exergy of exploited resources is calculated using Equation 4:

$$(Mb) = \sum_i z_i (Mb) i + \bar{R} T_0 \sum i z_i \ln z_i \tag{4}$$

Here, z_i represents the molar share of the i-th mineral in the resource, $(Mb)_i$ denotes the molar exergy of the i-th mineral in the resource, obtained via the Exergy-calculator [11]. The symbol $\bar{R}$ is the universal gas constant, and T_0 is the standard reference temperature (298 K). The nuclear exergy of uranium was considered to be 239.27 MJ/kg of ore, as noted in [9].

To calculate the TEC, a complete list of inputs and outputs from the LCA for Experts (GaBi) software was utilized. Given that such a matrix contains a large dataset, the following simplification was made: only inputs with a mass share above 0.5% in relation to the total mass entering the system were considered in the calculation, with the exception of the uranium source. For all considered cases, around 99% of the mass entering the system is included in the calculations, covering both energy and non-energy resources.

A key limitation of this methodology is the value of w_k, used in Equation 2, which requires knowledge of how the harmfulness of emissions from damaging substances can be quantified in monetary terms (i.e., EUR/kg). This quantification depends on multiple factors, and as a result, these indices are often limited to SO2, NOx, and PM emissions [9], [10]. In such form, the TEC of waste products was presented in the report M4.2. However, this report adopts a different approach since accounting solely for these emissions does not capture the decarbonization effect. In this work, it is assumed that w_k is represented by the prices set by the Minister of Climate and Environment of Poland on August 4, 2023, regarding the rates of charges for the use of the environment for the year 2024. Accordingly, the included emissions consider a broader range of pollutants: CO2, CH4, N2O, CO, NOx, NH3, SO2, PM, PAH, Cr, Pb, Hg, Ni, Zn, Cd, and Ar. While the direct exergy consumption part can be considered globally valid, the TEC of a waste product is calculated with reference to the Polish market.

The results of the TEC are presented in Figure 3.1. It is clear that the TEC results are predominantly influenced by the exergy consumption of the input streams. The grey, blue, and green PV ammonia options result in moderately higher TEC impacts compared to the reference case, with the green PV option showing approximately a 40% increase. Conversely, the green wind ammonia option demonstrates a lower thermo-ecological impact, with about a 30% reduction compared to the diesel case. The scenario using nuclear-based ammonia results in a nearly 400% increase in TEC impact. The green wind ammonia option emerges as the most favorable.

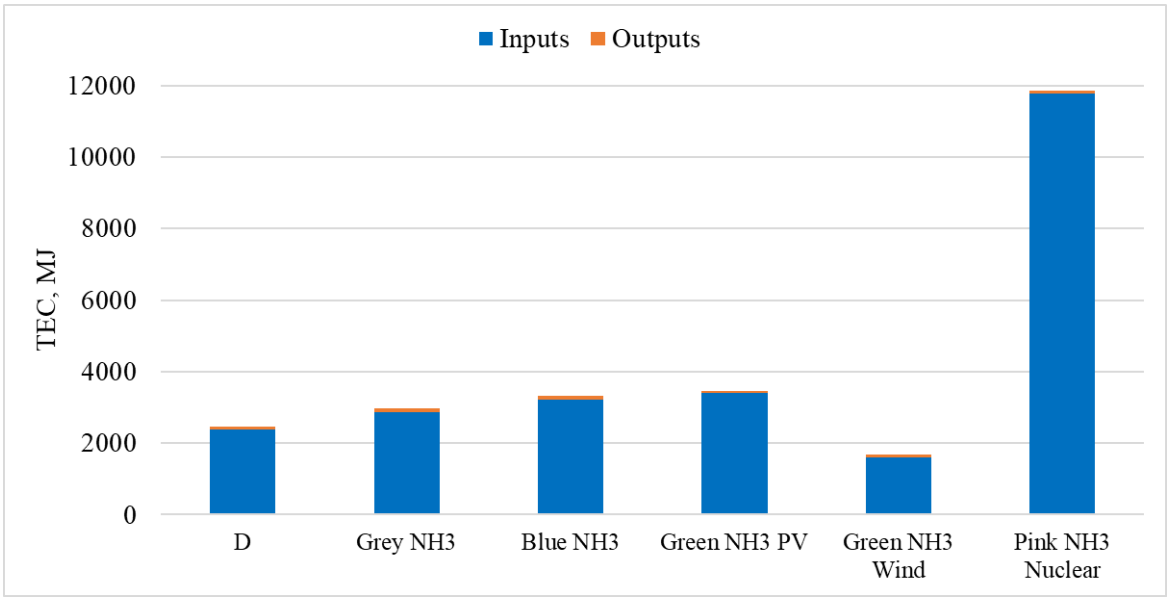

Figure 3.1: Thermo-ecological cost results.

4 Summary

The transition away from fossil fuels necessitates the use of carbon-free, renewable energy sources. An evaluation of the environmental impact of the ACTIVATEngine reveals that producing ammonia via electrolysis, powered by PV, wind, or nuclear energy, can reduce the impact on climate change

by approximately 15% compared to a diesel reference case. The modest decarbonization effect is primarily due to high emissions of N2O from ammonia combustion. Further research should therefore concentrate on advancing combustion optimization, enhancing exhaust gas treatment, or improving Selective Catalytic Reduction units to mitigate N2O emissions.

From a comprehensive Life Cycle Assessment standpoint, all ammonia-fueled scenarios are associated with a significantly higher environmental impact on human health and ecosystem quality. This is largely attributable to the high concentration of ammonia in the exhaust, despite its partial consumption in the SCR unit. Addressing this issue should be a priority for future research. In terms of the thermo-ecological cost — an indicator of the depletion of non-renewable natural resources and emissions — the use of wind energy for ammonia electrolysis in vehicles emerges as the most advantageous option.

The sustainability analysis of the ACTIVAEngine demonstrates the potential of ammonia as an alternative fuel for vehicles traditionally powered by diesel. However, to realize more substantial benefits, further refinement of the engine and exhaust treatment systems is recommended.

References

[1] Sergio Morais, Teresa Mata, António Martins, Gilberto Pinto, and Carlos Costa. Simulation and life cycle assessment of process design alternatives for biodiesel production from waste vegetable oils. *Journal of Cleaner Production*, 18:1251–1259, 09 2010. doi:10.1016/j.jclepro.2010.04.014.

[2] Camilla Sundin. Environmental assessment of electrolyzers for hydrogen gas production. *KTH Royal Institute of Technology School of Engineering Sciences in Chemistry, Biotechnology and Health*, page 4, 2019.

[3] University of Maine Lois Berg Stack. Calendar of apple orchard management activities from the gardenpro answer book, [online; accessed 30-november-2021]. URL: https://extension.umaine.edu/gardening/manual/calendar-apple-orchard-management-activities/.

[4] Elshout P.M.F. Stam G. Verones F. Vieira M.D.M. Hollander A. Zijp M. Van Zelm R Huijbregts M.A.J., Steinmann Z.J.N. Recipe 2016 v1.1 a harmonized life cycle impact assessment method at midpoint and endpoint level report i: Characterization. *National Institute for Public Healthand the Environment*, 2016.

[5] Kacper Kuta, Grzegorz Przybyła, Damian Kurzydym, and Zbigniew Żmudka. Experimental and numerical investigation of dual-fuel ci ammonia engine emissions and after-treatment with v2o5/sio2–tio2 scr. *Fuel*, 334:126523, 2023. URL: https://www.sciencedirect.com/science/article/pii/S0016236122033476, doi:https://doi.org/10.1016/j.fuel.2022.126523.

[6] Yongjin Jung, Youngdug Pyo, Jinyoung Jang, Youngmin Woo, Ahyun Ko, Gangchul Kim, Youngjin Shin, and Chongpyo Cho. Nitrous oxide in diesel aftertreatment systems including doc, dpf and urea-scr. *Fuel*, 310:122453, 2022. URL: https://www.sciencedirect.com/science/article/pii/S0016236121023243, doi:https://doi.org/10.1016/j.fuel.2021.122453.

[7] Mateusz Proniewicz, Karolina Petela, Andrzej Szlek, Grzegorz Przybyła, Ebrahim Nadimi, Łukasz Ziółkowski, Terese Løvås, and Wojciech Adamczyk. Energy and exergy assessments of a diesel-, biodiesel-, and ammonia-fueled compression ignition engine. *International Journal of Energy Research*, 2023:9920670, 2023. doi:10.1155/2023/9920670.

[8] Vishavdeep Singh, Ibrahim Dincer, and Marc Rosen. *Life Cycle Assessment of Ammonia Production Methods*, pages 935–959. 01 2018. doi:10.1016/B978-0-12-813734-5.00053-6.

[9] W. Stanek and Wydawnictwo Politechniki Ślaskiej. *Analiza egzergetyczna w teorii i praktyce*. Monografia - Politechnika Ślaska. Wydawnictwo Politechniki Ślaskiej, 2016. URL: https://books.google.pl/books?id=fJzsswEACAAJ.

[10] W. Stanek, P. Gladysz, L. Czarnowska, and T. Simla. *Thermo-ecology: Exergy as a Measure of Sustainability*. Elsevier Science, 2019. URL: https://books.google.pl/books?id=8AWVswEACAAJ.

[11] Exergoecology portal and exergy calculator. http://www.exergoecology.com/. Accessed: [20.11.2023].